Two in vivo surgical approaches for lumbar corpectomy using allograft and a metallic implant: a controlled clinical and biomechanical study

Philbert Huang, BS[a], Munish C. Gupta, MD[a], Nesrin Sarigul-Klijn, PhD[b,*], Scott Hazelwood, PhD[a]

[a]*Department of Orthopedic Surgery,* [b]*Mechanical and Aeronautical Engineering Department, University of California at Davis, 2132 Bainer Hall Drive, Davis, CA 95616-5294*

Abstract

BACKGROUND CONTEXT: Both bone graft and metallic implants have been used in combination with the necessary anterior rod or plate instrumentation to fill the voids left by vertebral body removal, with the ultimate goal of restoring stability. One type of device that has recently been introduced is an expandable titanium telescoping cage that is designed to be used as a strut implant to fill corpectomy defects. The use of these devices has met varying success. Acceptance by surgeons and spine biomechanicians has been limited by clinical failure with subsequent loss of reduction and increase in kyphosis. In order to further improve patient care, it is critical to evaluate the use of these implants through biomechanical as well as other modes of testing.

PURPOSE: To compare and contrast the spinal fusion outcome of using allograft bone versus the expandable vertebral body replacement titanium implant in a lumbar corpectomy procedure.

STUDY DESIGN: Controlled biomechanical study of lumbar spine fusion using bone graft and the expandable cage in an in vivo bovine model after a 4-month postoperative healing period (n=6).

ANIMAL MODEL: Twelve Holstein calves aged 4–6 months with L3 and adjacent discs removed to create a simulated lumbar corpectomy defect.

OUTCOME MEASURES: Lumbar spine stability after corpectomy repair was quantified by biomechanical parameters. Strength of fusion was assessed by stiffness of ex vivo spine specimens in flexion-extension, lateral bending, and torsion obtained from biomechanical testing. Uniaxial strain at various positions on the surface of the anterior plate was measured during loading as an additional stability parameter. Loading tests were repeated after removal of the anterior instrumentation (plate and the screws).

METHODS: The calves were randomly allocated to groups for corpectomy defect repair with 1) Allograft metatarsal bone and thoracolumbar spine locking plate, n=6; or 2) Expandable vertebral body replacement device, and thoracolumbar spine locking plate, n=6. After a 4-month postoperative period, anterior-posterior and lateral radiographs were taken of the spine, followed by animal sacrifice and harvesting of the lumbar spine for biomechanical and histological testing. For biomechanical testing, uniaxial strain gauges were applied to the thoracolumbar spine locking plate to measure plate deformation during loading in a custom built fixture for application of flexion-extension, lateral bending, and torsion moments in an Instron materials testing machine. These loading tests were repeated with the thoracolumbar spine locking plate removed, thereby loading solely the fused segment.

RESULTS: At 4 months postoperative, the stiffness of the calf spines repaired by the metatarsal allograft and thoracolumbar spine locking plate was significantly greater than that of the spines

repaired by the expandable cage and thoracolumbar spine locking plate. This finding was true for all three directions of loading (flexion-extension, left-right lateral bending, and torsion). Concordantly, the neutral zone, elastic zone, and range of motion of the spines repaired with the allograft bone were less than that of the spines repaired with the expandable cage. Greater strain values were observed from the gauges on the thoracolumbar spine locking plate of the spines using the expandable cage than the spines using allograft bone. This finding held for all gauge positions (anterior edge, anterior face, posterior edge, and posterior face at the longitudinal midpoint of the plate). After thoracolumbar spine locking plate removal and a repeat of the loading tests, a decrease in stiffness of the construct and a rise in the motion parameters were observed for both the allograft and cage groups.

CONCLUSIONS: The use of allograft bone for corpectomy defect repair in the lumbar spine appears to contribute to a stiffer and perhaps more stable spine segment compared with using the expandable cage device for such a repair after a 4-month healing period in this in vivo calf model. These findings thus far are based upon the biomechanical data gathered.

.

Keywords: Spinal disorders; Implants; Biomechanics; Grafts; Expandable cages

Introduction

Fractures, tumors, bacterial infections, and other diseases affecting one or more vertebral bodies can result in spinal instability or neural impingement. For many of these conditions it is necessary to reconstruct the destabilized spine after anterior decompression of the spinal cord by complete removal of the vertebral body, or vertebral corpectomy. Anterior bone grafting is often performed in combination with either anterior or posterior spinal instrumentation for the restoration of vertebral column stability. This stability is achieved over time via spinal fusion, during which the graft and plate construct provide an environment that encourages the formation of a bony bridge across the graft–host vertebral body interfaces.

It is believed that the use of autologous graft still remains the gold standard [1]. However, obtaining an appropriate strut graft through the harvesting of autologous bone sources does have some shortcomings. Disadvantages include pain, neural injury, loss of structural support, risk of soft-tissue herniation, and infection [2]. In some situations, the amount of tissue required to repair a bony void is unable to be filled by commonly used autologous sources, in which case alternative grafting sources would be required. This finding is especially true in the lumbar region where relatively larger defect spaces must be filled. Disadvantages of allograft bone usage include longer initial fusion times, slower and diminished vascular penetration, immunologic rejection by the host, and in rare cases, the risk of disease transmission [3]. It is apparent that neither allograft nor autograft is the ideal reconstructive material in all circumstances concerning corpectomy.

Recently, several synthetic vertebral body replacement devices made of titanium and other materials have become popular substitutes for structural bone grafts. These implants provide axial load-bearing capability, and often have a central canal through which morselized bone can be inserted, similar to the technique used for allograft bone. Thus, large cortico-cancellous bone grafts traditionally used in surgery are not needed [4]. The potential advantages of these ''cage'' devices in anterior spinal reconstruction for trauma are the wide variety of graft shapes and sizes to choose from and the absence or minimization of donor site morbidity in the case of autogenous iliac crest graft.

One such device is an expandable vertebral body replacement implant. It is manufactured from a titanium alloy (Ti-6Al-7Nb) and consists of two telescoping cylinders that can be adjusted to a finite number of heights by unlocking a ring with a dedicated tool. The center is hollow to allow the insertion of bone pieces, and the ends of the cylinders are characterized by small holes allowing for some contact of the bone housed within the cylinders with the bone packed outside the cylinder as well as the vertebral end plate. The ends of the cylinders are also designed with a footprint for stability once placed in position between the vertebrae.

The thoracolumbar spine locking plate system consists of a range of plate sizes and 5.5-mm cancellous screws with a locking head. The plates attach to the anterolateral aspect of the vertebral body of the thoracolumbar spine (levels T1–L5) for the purpose of stabilization to permit the biological process of spinal fusion to occur. All components are manufactured from titanium alloy. The use of this plate is indicated for use via the lateral or anterolateral surgical approach in the treatment of thoracic and thoracolumbar (T1–L5) spine instability as a result of fracture, tumor, scoliosis, kyphosis, or a failed previous spine surgery.

In vitro biomechanical testing of these devices has yielded mixed results. Recurrent instability can be caused by mechanical failure, by a loosening at the interface between implant and bone, or by a metastatic relapse. Metallic implants used in the past have frequently disturbed postoperative computed tomography (CT) or magnetic resonance imaging (MRI) due to artifacts, and they have also interfered with the planning and administration of radiotherapy [4]. Some biomechanical studies have indicated that torsional stability may not be achieved adequately even with rigid fixation devices [5]. With regard to allograft, full

incorporation can take a long time. Occasionally, pseudarthrosis and mechanical failure can be observed during the first two years [4]. Because it is important to perform evaluations in the context of the natural healing abilities of soft tissue and bone, we believe an in vivo study would be ideal and will allow for ex vivo radiographic, biomechanical, and histological analysis. We propose an in vivo and ex vivo investigation of the efficacy of the cage device used with the locking plate versus the bone graft with locking plate in contributing to a successful spinal fusion after a lumbar corpectomy procedure. The biomechanical results are presented in this paper together with the details of the surgical procedures.

Animal models and methods

An accurate clinical assessment of fusion is challenging, partly because only noninvasive evaluation techniques are available. Animal models permit a systematic and objective evaluation of spinal fusion because of the ability to analyze the constructs mechanically and histologically [6]. Modeling spine surgical procedures in animals also allows for standardization of procedure to better compare outcomes of different treatment options. As new devices are designed and marketed to improve spine fusion and reconstruction outcomes, in vivo animal models for implant incorporation studies become increasingly important to validate their efficacy.

Study group

Twelve male Holstein calves of age 4 to 6 weeks were used in this study following animal use and care protocol approval by the local institutional animal care and use committee. Two calves were used during pilot studies to perfect the surgical technique in this species. From the first calf we harvested with sterile technique both the left and right tibial and metatarsal bones from the hind limbs. Bone excision was achieved with the use of both a hand-operated Gigli saw and a gas-powered oscillating saw. The resulting bone segments were then wrapped in saline- and cefazolin-soaked gauze, double-bagged, and stored at -20° Celsius. In this terminal-procedure calf we also performed a complete corpectomy procedure with expandable cage and locking plate to become familiar with the approach, blood loss, anesthesia, and vertebral body defect size. On an additional pilot animal, a complete corpectomy procedure was performed with the expandable cage and thoracolumbar spine locking plate. This animal was recovered from the surgery and was observed over a 4-month postoperative period to ensure that there were no complications which would adversely affect animal well-being. The animals for both experimental groups were brought to the site of the surgery 1 week before the date of the scheduled procedure to allow for acclimation. Feeding was held for 12 hours before the procedure, but water was still available for the animals during the fast.

Fig. 1. Metatarsal allograft placed within corpectomy defect in the calf spine.

Operative procedure

For both experimental groups, anesthesia was induced with Xylazine 0.1 mg/kg intravenously. This produced adequate relaxation to facilitate inserting an intravenous catheter into the jugular vein. Ketamine 3 mg/kg was given to effect in order to intubate with a cuffed endotracheal tube of appropriate size (depending upon the weight of the calf). Anesthesia was then maintained with 1–3% volatilized isoflurane until the end of the procedure. The calves were given a maintenance infusion of lactated Ringer's solution at a rate of 10 cc/kg/hr for the first hour, followed by 5 cc/kg/hr afterwards. In a lateral position, each calf's right flank was shaved, then prepared with betadine scrub, and the surgical site was appropriately draped. Using sterile technique, an anterior retroperitoneal approach to the lumbar spine was utilized through a curvilinear skin incision from the level of the upper lumbar spine down to the level of the lumbosacral junction. Once adequate exposure of the L2–L4 spine segment was obtained, the segmental vessels were ligated and a corpectomy of L3 was performed.

Fig. 2. Expandable cage consisting of two telescoping pieces with footprint and central canal distracted within the corpectomy defect.

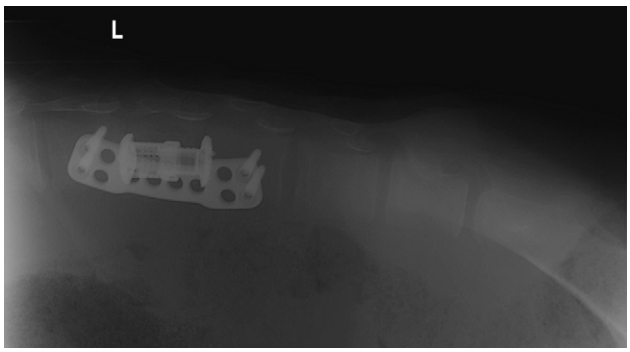

Fig. 3. A 3-month postoperative lateral X-ray of lumbar calf spine instrumented with expandable cage and locking plate.

The L3 body and adjacent intervertebral discs were marked with the scalpel and cautery. Using rongeurs, the adjacent discs were removed. Using an osteotome and hammer, a large section of the vertebral body was removed. Stopping bone bleeds was facilitated by the use of bone wax. The remaining pieces of vertebral body and disc were scraped away and removed with curettes. The posterior wall, or posterior portion of the middle column of the vertebral body was left intact to protect the spinal cord. The end plates were also scraped with the curettes to remove all fibrocartilaginous disc tissue so bony contact with the bone graft or implant occurred. The cortical and trabecular bone from the excised vertebral body was saved and cut into smaller pieces using the rongeurs.

For the bone graft group, the tibial and metatarsal allografts previously harvested were thawed in normal saline. Once thawed, the bone graft was measured and appropriately cut to size with the oscillating saw. The hollow medullary canal of the cortical allograft was packed with local cortical and cancellous bone chips from the excised L3 vertebra. This packed allograft was then placed in the space of the removed L3 vertebral body (Fig. 1). Distraction of the defect

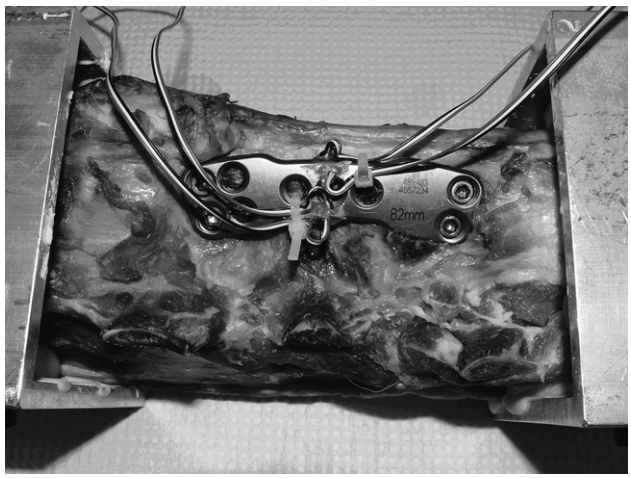

Fig. 5. Lateral view of the locking plate with strain gauges attached to anterior and posterior face.

space before graft placement was achieved by applying an external force directed ventrally against the back of the animal at the level of the corpectomy. An adequate compression fit was achieved by gently hammering in the allograft as assessed by the operating surgeon, an attending spine orthopedist. The space around the allograft was then also packed with remaining bone chips from the excised vertebral body. After insertion of the allograft strut, the construct was stabilized with an appropriately sized locking plate device using two titanium cancellous locking screws in L2 and two screws in L4 in accordance with the guidelines.

Calves in the expandable cage group underwent the same anterior procedure but had an appropriately sized expandable vertebral body replacement device placed and appropriately distracted in the L3 vertebral body space in conjunction with the locking plate device (Fig. 2). The ends of the expandable cage were packed with autogenous bone chips before insertion, and the central canal of the cage was

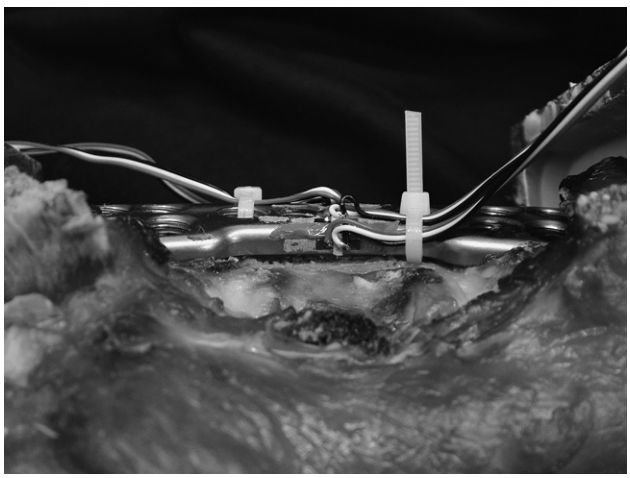

Fig. 4. Posterior view of the locking plate showing strain gauge attached to posterior edge.

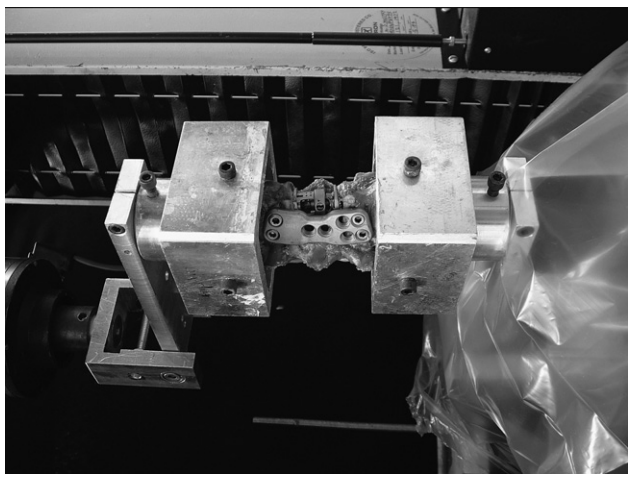

Fig 6. Calf spine instrumented with expandable cage and locking plate mounted in flexion-extension/lateral bending loading fixture.

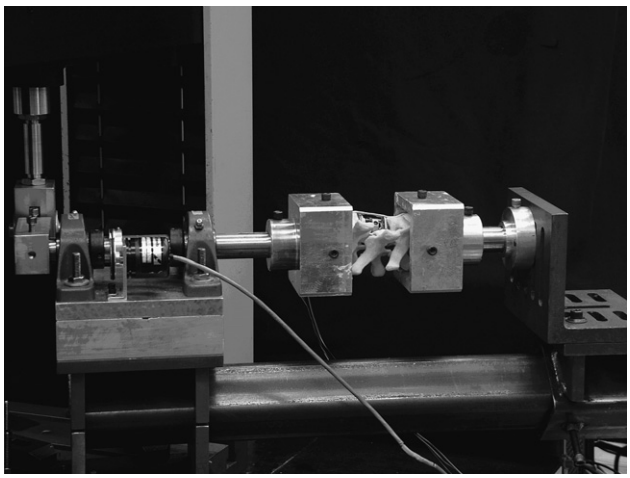

Fig. 7. Torsion fixture showing fixed end at right and rotating end attached to Instron crosshead at left. Also shown is a rotary variable inductance transducer used to measure angular displacement.

packed with bone after insertion and distraction. Bone fragments were also placed in the area surrounding the cage before plate application. After completion of the instrumentation, the surgery site was cleaned and irrigated with saline. All calves were also castrated after the completion of the spinal procedure for reduction of aggression and ease of handling during the postoperative period. The animals were then taken to the adjacent imaging room for fluoroscopy so that anterior-posterior and lateral X-rays could be taken. For postoperative care, the animals received analgesics and antibiotics and were monitored continuously for vitals until they were able to stand unassisted. Once stable, the animals were left free to move about within the confines of a 535-square-foot isolation unit housed in a barn, and then returned to outdoor pens with ad libitum activity if the attending veterinarian agreed. After a 4-month survival period, the animals were euthanized and the spines were harvested for ex vivo fusion evaluation. Analysis for spinal fusion included radiographic evaluation (Fig. 3), biomechanical testing, and histology.

Biomechanical testing

After harvest, the spines were stored in a freezer at −20°C. Before testing, the frozen specimens were thawed at room temperature, and the paraspinal soft tissue was removed to obtain the ligamentous spinal specimen (L1–L5). The locking plate was prepared so that four uniaxial strain gauges (model EA-05-031DE-350; Measurements Group, Raleigh, North Carolina) could be attached to its surface at the middle of the plate. The four locations of the strain gauges included 1) anterior edge of the plate, 2) anterior region of the outwardly directed face of the plate, 3) posterior region of the outwardly directed face of the plate, and 4) posterior edge of the plate. The strain gauges on the edges of the plate were placed to primarily detect deflection during flexion-extension-type movements as shown in Figure 4, and the strain gauges on the face of the plate were placed to primarily detect deflection during lateral bending-type movements (Fig. 5).

The L1 to L5 spinal column segments were then embedded in aluminum pots designed to fit into the testing apparatus using polymethylmethacrylate. To protect against drying out during the tests, the specimens were loosely wrapped in moistened gauze. To further ensure moist conditions, the specimen were sprayed intermittently with 0.9% saline. Each specimen was mounted in a loading frame in an Instron 5800R (Instron, Canton, MA) testing machine for loading in flexion, extension, as shown in Figure 6, and left/right lateral bending [7]. Following the criteria outlined by Wilke et al., the specimen was loaded in the positive and negative directions continuously (anterior-posterior or left-right) in order to obtain load-displacement curves that reflect the full cycle

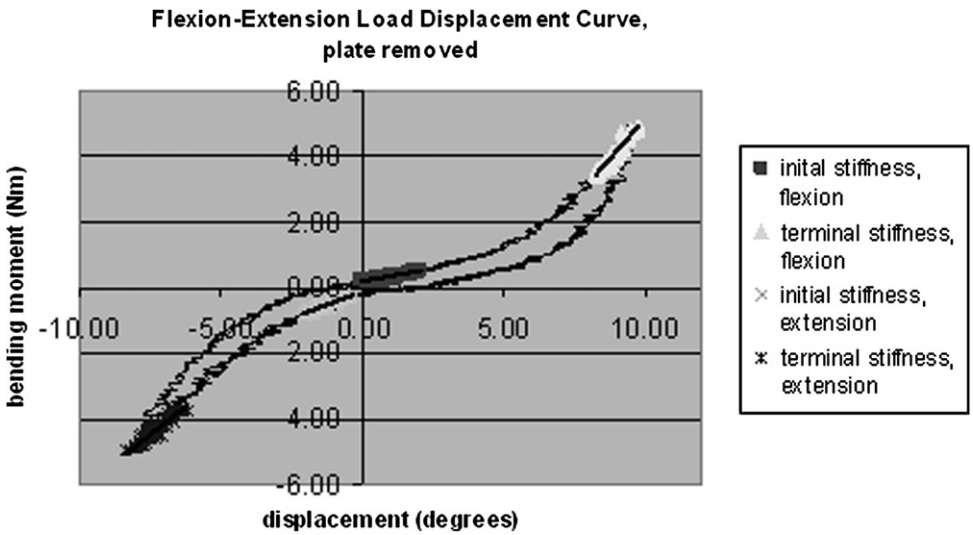

Fig. 8. Example of load-displacement curve of lumbar spine segment repaired with expandable cage in three cycles of 5 Nm flexion-extension with thoracolumbar spine locking plate removed. Highlighted are the initial and terminal stiffness obtained from the loading curve.

Table 1
Stiffness (Nm/deg) of lumbar segment repaired with bone graft versus expadable cage

	Bone graft		Cage	
Construct with plate	Initial stiffness	Terminal stiffness	Initial stiffness	Terminal stiffness
Flexion	0.80±0.58	1.49±0.20	0.22±0.08	1.21±0.12
Extension	0.84±0.38	1.38±0.13	0.47±0.15	0.94±0.10
Right lateral bending	0.14±0.04	1.13±0.50	0.09±0.04	0.78±0.06
Left lateral bending	0.31±0.17	1.33±0.49	0.14±0.07	1.05±0.15
CCW torsion	2.80±0.53	3.43±0.77	1.24±0.61	1.80±0.38
CW torsion	2.61±1.17	3.74±2.25	1.27±0.50	1.86±0.78

CCW=counterclockwise; CW=clockwise.

of motion in a given direction [8]. For flexion-extension and left-right lateral bending, two rotational transducers (DC-operated rotary variable inductance transducers) were used to measure angular displacement from the offset arms of the loading frame. An Instron load cell (5 kN) affixed to the offset arm (superior mounting pot of the specimen) was used to measure the applied force, and the bending moment was calculated as the product of force and length of the offset arm. Applying an axial torque to the spine specimens was achieved in a similar manner using a dedicated torsion apparatus (Fig. 7). The caudal end of the spine segment was secured in the fixed end of the fixture, while the cranial end was placed at a freely rotating end attached to a moment arm that could be actuated by the Instron testing machine crosshead. Loading was carried out at a speed of 2 mm/s for all loading directions.

Results

At 4 months postoperative, the stiffness of the calf spines repaired by the metatarsal allograft and locking plate was significantly greater than the spines repaired by the expandable cage and locking plate. This finding was true for all three directions of loading (flexion-extension, left lateral bending, and torsion). Concordantly, the neutral zone, elastic zone, and range of motion were smaller in the spines repaired with the allograft bone compared with the spines repaired with the expandable cage. Greater strain values were seen from the gages on the locking plate of the spines using the expandable cage than the spines using allograft bone. This finding was true for all gauge positions (anterior edge, anterior face, posterior edge, and posterior face at the longitudinal midpoint of the plate).

Load displacement curves

The load displacement curves obtained from biomechanical testing all displayed a distinguishable amount of hysteresis, indicating the viscoelastic nature of the spine. There was not an appreciable difference in the hysteresis curves of the two preconditioning cycles and the third cycle used for data analysis. For flexion-extension and lateral bending, the curves have a characteristic ‘‘toe’’ region, which corresponds to limits in the physiological range in flexibility of the instrumented specimen. The initial stiffness corresponds to the normal physiologic range of motion that the spine undergoes, which is a function of the disc mechanical properties and bony structures that limit movement in certain directions. A somewhat abrupt change in slope is evident in both the flexion-extension and lateral bending curves, which reflects the transition from initial stiffness to terminal stiffness. In the terminal stiffness region, the limits of the normal range are encountered during which the plate and strut construct begin to experience load and deformation (Fig. 8). The testing in torsion displayed less of a distinct initial and terminal stiffness, which is most likely attributable to the increased stiffness in this mode of loading.

Upon inspection of the curves, it is generally evident that a greater range of motion is present in flexion over extension. This finding is attributable to the anatomical characteristics of the spine in the lumbar region that limit motion in the extension direction. In extension, motion is primarily limited by the intervertebral facet joints and

Table 2
Stiffness (Nm/deg) of lumbar segment repaired with bone graft versus expandable cage after plate removal

	Bone graft		Cage	
Construct with plate removed	Initial stiffness	Terminal stiffness	Initial stiffness	Terminal stiffness
Flexion	0.62±0.50	1.42±0.28	0.14±0.04	0.98±0.19
Extension	0.96±0.21	1.49±0.18	0.39±0.11	0.87±0.15
Right lateral bending	0.14±0.11	0.86±0.17	0.08±0.02	0.69±0.04
Left lateral bending	0.40±0.28	1.21±0.14	0.12±0.07	0.98±0.26
CCW torsion	2.47±0.79	3.67±0.66	1.01±0.36	1.95±0.40
CW torsion	2.84±0.85	3.43±0.76	1.04±0.25	1.61±0.28

CCW=counterclockwise; CW=clockwise.

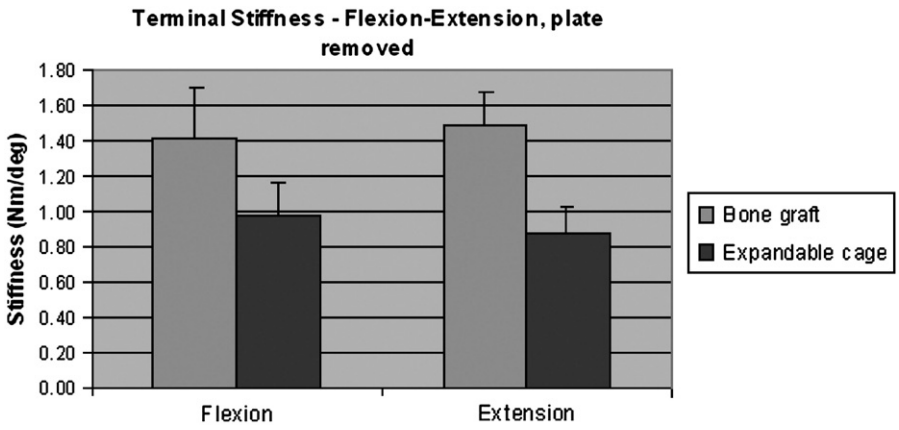

Fig. 9. Terminal stiffness of a five-level bovine lumbar spine segment repaired with bone graft versus expandable cage in flexion-extension. Data taken from third cycle of 5-Nm maximum loading with thoracolumbar spine locking plate removed.

anterior longitudinal ligament. In flexion, motion is limited by the posterior longitudinal ligament and the interspinous ligaments. The same can be said for lateral bending on the right side as opposed to the left. This discrepancy may be attributed to the axial compressive and bending moment loads that the right side was subjected to during the testing, as well as the asymmetric nature of the placement of the thoracolumbar spine locking plate, which is situated on the right anterior aspect of the spine. The torsion curves are for the most part symmetric with respect to left and right axial movements. After removal of the plate and a repeat of the loading protocol in the three directions, an expected increase in the range of motion in all directions was observed for both the allograft and cage group.

Stiffness effects

At 4 months postoperative, the stiffness of the calf spines repaired by the metatarsal allograft and thoracolumbar spine locking plate was significantly greater than the spines repaired by the titanium cage and thoracolumbar spine locking plate. This finding was true for all three directions of loading (flexion-extension, left lateral bending, and torsion), as summarized in Tables 1 and 2. All data in tables are presented as mean value ± standard deviation. The results show that the stiffness was greater for the allograft construct than the cage construct when the anterior instrumentation thoracolumbar spine locking plate was removed and the loading tests repeated (Fig. 9).

Motion parameters

Concordant with the stiffness differences, the neutral zone, elastic zone, and range of motion were smaller in the spines repaired with the allograft bone compared with the spines repaired with the titanium cage (Fig. 10). After removal of the plate, the same trend was observed (Tables 3 and 4).

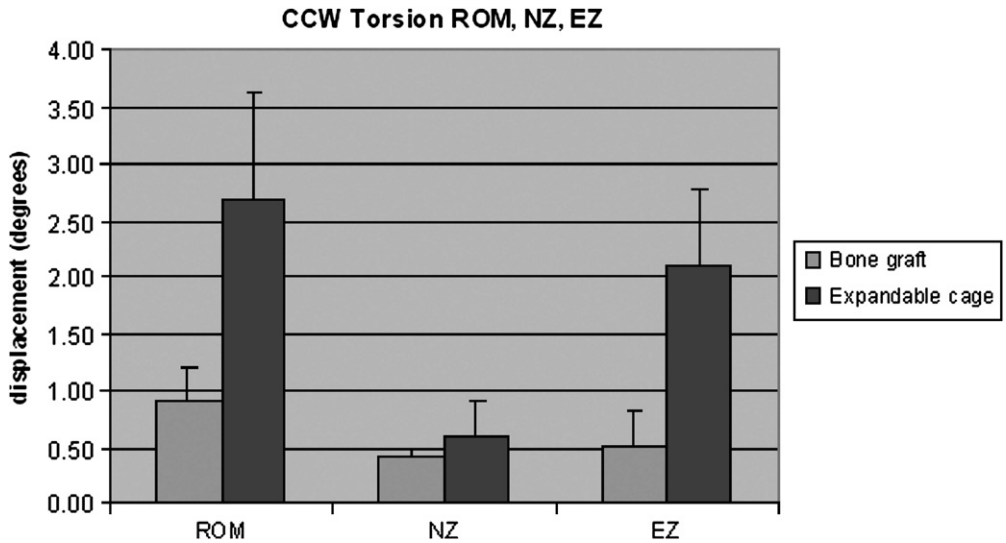

Fig. 10. Range of motion (ROM), neutral zone (NZ), and elastic zone (EZ) of a five-level bovine lumbar spine segment repaired with bone graft versus expandable cage in counterclockwise (CCW) torsion. Data taken from the third cycle of 5 Nm maximum loading with thoracolumbar spine locking plate intact.

Table 3
Motion parameters (degrees) of bone graft versus cage under 5 Nm of loading

	Bone graft			Cage		
Construct with plate	ROM	NZ	EZ	ROM	NZ	EZ
Flexion	4.56±0.03	0.99±0.76	3.57±1.48	8.30±1.98	1.12±0.86	7.18±1.46
Extension	3.76±0.82	0.62±0.31	3.13±0.88	6.35±1.24	1.08±0.29	5.27±1.02
Right lateral bending	9.57±3.07	2.24±1.82	7.33±2.35	12.97±1.41	3.11±0.67	9.86±1.14
Left lateral bending	6.11±1.97	2.16±0.74	3.95±1.45	9.14±1.71	1.75±1.03	7.39±1.47
CCW torsion	0.92±0.15	0.40±0.29	0.52±0.21	2.69±1.02	0.59±0.30	2.10±0.84
CW torsion	0.83±0.28	0.27±0.09	0.56±0.30	2.10±0.92	0.47±0.32	1.63±0.65

ROM=range of motion; NZ=neutral zone; EZ=elastic zone; CCW=counterclockwise; CW=clockwise.

Strain distribution

Greater strain values were seen from the gauges on the thoracolumbar spine locking plate of the spines using the titanium cage than the spines using allograft bone. This finding was for the most part true for all gauge positions (Fig. 11) (anterior edge, anterior face, posterior edge, posterior face at the longitudinal midpoint of the plate), with a few exceptions. There was no significant difference in maximum strain values recorded on the anterior and posterior face for the allograft versus cage group, as summarized in Tables 5 and 6. This may indicate that the strength to resist loads causing tensile forces on the plate surface was similar in both groups.

Statistical analysis

Statistical analysis was carried out using the single-factor analysis of variance model I with α=.05. Differences found between response variables with the F test were further characterized with the Tukey multiple comparison procedure at α=.05 and 95% confidence intervals.

Discussion

This is the first in vivo bovine model study comparing allograft bone and a titanium implant in combination with an anterior plate for vertebral body replacement after a corpectomy procedure at the lumbar level. The use of allograft bone for corpectomy defect repair in the lumbar spine appeared to contribute to a stiffer and perhaps more stable spine segment compared with using the titanium cage implants for such a repair after a 4-month healing period in this model. These findings thus far are based upon the biomechanical data gathered.

The use of autograft bone in these types of repair procedures in the spine has been considered the ''gold standard'' largely due to the graft's osteoconductivity and adequate strength when cortical bone types are used. It is intuitive that a strut composed entirely of bone would facilitate bone in-growth and healing. Perhaps these attributes also hold in the bovine model. The modulus of cortical bone is significantly less than that of the titanium alloy from which the expandable cage is manufactured, which may allow for slightly more ''give'' or micro-motion in the bone graft construct during the healing process. It has been observed that the rate of healing and the extent of callus formation in secondary or typical fracture healing can be modulated by the mechanical conditions at the fracture site [9]. It has also been shown that the repair process can be retarded under conditions of insufficient mechanical stimulation. This process may confer an advantage of the bone graft over the cage by reducing stress-shielding effects.

Kanayama et al. [10] compared the construct stiffness afforded by 11 differently designed lumbar interbody fusion devices and quantified their stress-shielding effects by measuring pressure within the devices. From an examination of the relationship between stress shielding and cage design, the correlation analysis the authors performed showed that the stress-shielding effect was better correlated to the largest pore size of the cage than to the total porous area. The authors also concluded that if two different cages have the same equivalent total porous surface area, then the cage with the larger contiguous pore produces less

Table 4
Motion parameters (degrees) of bone graft versus cage under 5 Nm of loading after plate removal

	Bone graft			Cage		
Construct with plate removed	ROM	NZ	EZ	ROM	NZ	EZ
Flexion	5.73±2.94	0.53±0.20	5.19±2.94	10.81±2.78	1.05±0.61	9.77±3.32
Extension	3.48±0.76	0.79±0.36	2.69±0.51	7.45±1.53	1.76±1.10	5.68±1.00
Right lateral bending	11.43±1.50	2.60±1.68	8.83±2.60	14.48±1.47	2.59±0.93	11.89±1.82
Left lateral bending	5.38±1.52	1.78±0.77	3.60±1.11	10.57±2.36	2.39±1.22	8.18±2.81
CCW torsion	0.96±0.20	0.27±0.12	0.69±0.17	2.90±0.94	0.63±0.13	2.27±0.91
CW torsion	0.84±0.13	0.26±0.08	0.59±0.19	2.16±0.73	0.45±0.17	1.72±0.57

ROM=range of motion; NZ=neutral zone; EZ=elastic zone; CCW=counterclockwise; CW=clockwise.

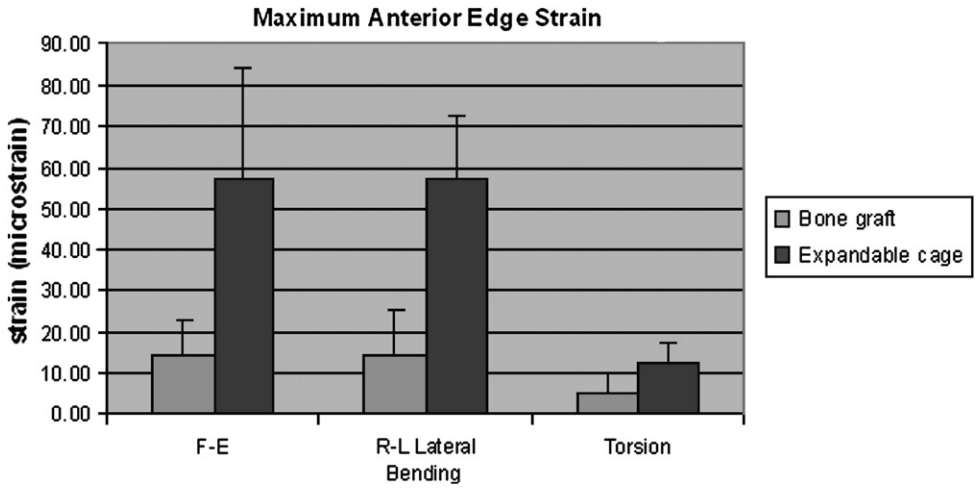

Fig. 11. Maximum positive (tensile) strain on the surface of the anterior edge of the thoracolumbar spine locking plate at the midline in flexion-extension (F-E), right-left (R-L) lateral bending, and torsion. These strain values represent the maximum of all three 5-Nm loading cycles.

stress-shielding than that with several smaller pores. With respect to fusion, the large central pore of the allograft bone may have been advantageous over the multiple small holes characteristic of the titanium cage.

Along the same lines, Steffen et al. [11] believe that for successful fusion to occur, it appears logical to strive for the smallest possible cage volume (large inner/outer diameter ratio) so that more graft material can be packed into the prepared void space. The larger the contact surface area between bone graft and a properly prepared vertebral end plate, the more likely fusion may be. However, there may be a tradeoff between minimizing the cage contact area with the bony end plate and maximizing the graft–host bone contact area to increase the likelihood of a solid fusion. Having minimal contact between the graft or cage and the vertebral end plate may increase the risk of unwanted implant subsidence and contribute to graft/cage failure. Although the expandable cage may offer less bone–end plate contact, the in situ distraction that is achievable by such devices may also maximize stability by tensioning the ligamentous apparatus of the spine.

There is experimental evidence that autologous cancellous fragments could be used to set up centers of osteogenesis in sites where new bone formation is required. The formation of new bone seen in association with transplanted cancellous chips was further determined to not be induced bone, but rather bone formed from the osteogenic cells that covered or lined the chips [12]. Although the hollow centers of both the bone graft and the cage were packed with bone chips saved from the excised vertebral body, the geometry of the ends of the devices and subsequent exposure of the chips to the adjacent end plate may have dictated the efficacy of bone packing in each group. The allograft's hollow cylindrical shell shape was perhaps able to expose more cancellous bone chips to the end plate than the titanium cage ends, which are characterized by a pattern of small holes surrounded by a stabilizing footprint.

A limitation of the current study is the validity of using a calf for an in vivo model of a human spinal implant construct. The loads seen at the lumbar level of a quadruped may be dissimilar to that of the human that stands upright and is bipedal. Anatomical differences may also exist that may make the model less valid. An important finding that may be relevant to the current study is the bovine's 23% greater inter-transverse length at level L3, which is attributed to the very long transverse process at this level. This greater length is a factor that could influence the motion at each vertebral segment.

Further sources of error involve issues of animal age and postoperative healing time. Four- to 6-month-old calves

Table 5
Maximum and minimum strain (microstrain) at four locations on plate for bone graft construct

	Anterior edge		Anterior face		Posterior face		Posterior edge	
Bone graft	min	max	min	max	min	max	min	max
F-E	−10.74±4.94	14.61±7.88	−4.45±4.72	24.88±15.71	−6.26±6.52	11.93±7.47	−11.87±6.49	7.70±2.70
R-L bending	−13.37±13.87	14.36±10.96	−7.84±4.55	32.15±25.55	−36.16±24.13	42.98±34.36	−20.03±13.07	16.05±10.36
L-R rotation	−5.79±4.06	5.31±4.52	−2.23±2.04	12.64±10.12	−3.74±3.04	8.43±4.25	−6.07±2.51	4.15±4.98

F-E=flexion-extension; R-L=right-left; L-R=left-right.

Table 6
Maximum and minimum strain (microstrain) at four locations on plate for cage construct

	Anterior edge		Anterior face		Posterior face		Posterior edge	
Cage	min	max	min	max	min	max	min	max
F-E	−12.50±3.22	57.10±26.95	−63.70±45.31	20.49±14.55	−70.23±44.58	14.63±5.30	−5.08±2.85	40.40±88.99
R-L bending	−10.76±10.94	56.64±15.85	−91.70±54.25	32.10±29.81	−130.88±54.06	48.94±33.31	−16.95±16.30	47.56±32.34
L-R rotation	−9.58±8.38	12.18±5.32	−10.43±9.19	11.46±9.38	−12.91±13.76	9.90±6.59	−6.05±5.03	5.31±3.71

F-E=flexion-extension; R-L=right-left; L-R=left-right.

were chosen primarily for the appropriateness of spine size at this age in relationship to the size of implants that are typically used for humans. At this age, bone healing and repair is rather robust, and any differences in the extent of fusion using two different techniques may have been masked by such abilities to repair. The results may have differed for a more skeletally mature animal model. It remains to be defined how long a postoperative period is appropriate for complete fusion to occur and subsequent stability to be achieved. Previous in vivo spine fusion studies have typically used 4–6 months. Allowing for a longer postoperative repair/healing period may have yielded different results. It is plausible that the allograft strut may have contributed to a faster healing rate than the titanium cage during a 4-month postoperative period, which would be consistent with our results. If, however, a longer healing time was chosen, the titanium cage, although taking more time to heal, may have eventually contributed to fusion and less of a difference would have been observed between the two groups.

There are several studies that have analyzed the use of allograft in vivo and the use of some of the bone graft alternatives in vitro. The use of the expandable cage was analyzed by Knop et al. [13], for repairing a corpectomy of L1 in a human cadaveric model. Also, a human cadaveric study [14] made biomechanical comparisons between intact, autogenous bone graft, mesh titanium cage, and expandable cage constructs for the cervical spine. They found that expandable cages have no biomechanical advantage [15]. The authors later performed a similar study comparing expandable and nonexpandable devices in a human cadaveric L1 corpectomy defect model. From biomechanical testing the authors again concluded that design variations of expandable cages are of little importance [16]. These data are consistent with the inability of the expandable cage to achieve greater stiffness in the ex vivo specimens of the current study.

There have also been studies focusing on the variety of anterior instrumentation systems available. In a study of 12 anterior instrumentation systems including a device similar to the locking plate, Kotani et al. [17] performed static and fatigue biomechanical testing using mechanical testing standardized ultra-high molecular weight polyethylene cylinders machined to represent vertebral elements. They found that overall there were no substantial differences in stiffness (static testing) between rod devices and plate devices, but there were differences in fatigue testing.

Our current study examined fusion properties at just the 4-month postimplantation time point. Fatigue issues regarding the anterior plate would be important to consider for long-term efficacy in future studies. The stiffness of a five-level human lumbar spine segment under flexion-extension, left-right lateral bending, and torsion that corresponds to clinical stability has yet to be determined. Stiffness and stability in the spine are closely related, and it is plausible that such a stiffness value does exist that marks the transition from instability to stability. In the present study we compared the construct biomechanical properties of an expandable cage versus bone graft in repairing lumbar corpectomy defects in an in vivo bovine model. Our results indicate that after a 4-month postoperative period, the spine using bone graft repair was stiffer than that using the expandable cage. Further analysis of the radiographic and histological data may reveal if these stiffness differences truly indicate a difference in the extent of fusion and stability that is achieved.

References

[1] Riew DK, Rhee JM. The use of titanium mesh cages in the cervical spine. Clin Orthop 2002;394:47–54.

[2] Bridwell KH, Lenke LG, McEnery KW, Baldus C, Blanke K. Anterior fresh frozen structural allografts in the thoracic and lumbar spine. Do they work if combined with posterior fusion and instrumentation in adult patients with kyphosis or anterior column defects? Spine 1995;20:1410–8.

[3] An HS, Lynch K, Toth J. Prospective comparison of autograft vs. allograft for adult posterolateral lumbar spine fusion: differences among freeze-dried, frozen, and mixed grafts. J Spinal Disord 1995; 8:131–5.

[4] Eck KR, Lenke LG, Bridwell KH, Gilula LA, Lashgari CJ, Riew KD. Radiograph assessment of anterior titanium mesh cages. J Spinal Disord 2000;13:501–9; discussion 510.

[5] Lee SW, Lim TH, You JW, An HS. Biomechanical effect of anterior grafting devices on the rotational stability of spinal constructs. J Spinal Disord 2000;13:150–5.

[6] Steffen T, Marchesi D, Aebi M. Posterolateral and anterior interbody spinal fusion models in the sheep. Clin Orthop Relat Res 2000;371: 28–37.

[7] Chiba M, McLain RF, Yerby SA, Moseley TA, Smith TS, Benson DR. Short-segment pedicle instrumentation: biomechanical analysis of supplemental hook fixation. Spine 1996;21:288–94.

[8] Wilke HJ, Jungkunz B, Wenger K, Claes LE. Spinal segment range of motion as a function of in vitro test conditions: effects of exposure period, accumulated cycles, angular-deformation rate, and moisture condition. Anat Rec 1998;251:15–9.

[9] Goodship AE, Cunningham JL, Kenwright J. Strain rate and timing of stimulation in mechanical modulation of fracture healing. Clin Orthop Relat Res 1998;355(Suppl):S105–15.

[10] Kanayama M, Cunningham BW, Haggerty CJ, Abumi K, Kaneda K, McAfee PC. In vitro biomechanical investigation of the stability and stress-shielding effect of lumbar interbody fusion devices. J Neurosurg 2000;93(2 Suppl):259–65.

[11] Steffen T, Tsantrizos A, Fruth I, Aebi M. Cages: designs and concepts. Eur Spine J 2000;9(Suppl 1):S89–94.

[12] Ham, Arthur W. Histology. Philadelphia: J.B. Lippincott, 1974.

[13] Knop C, Lange U, Bastian L, Blauth M. Three-dimensional motion analysis with Synex. Comparative biomechanical test series with a new vertebral body replacement for the thoracolumbar spine. Eur Spine J 2000;9:472–85.

[14] Kanayama M, Cunningham BW, Weis JC, Parker LM, Kaneda K, McAfee PC. Maturation of the posterolateral spinal fusion and its effect on load-sharing of spinal instrumentation. An in vivo sheep model. J Bone Joint Surg Am 1997;79:1710–20.

[15] Kanayama M, Hashimoto T, Shigenobu K, Oha F, Ishida T, Yamane S. Pitfalls of anterior cervical fusion using titanium mesh and local autograft. J Spinal Disord Tech 2003;16:513–8.

[16] Pflugmacher R, Schleicher P, Schaefer J, et al. Biomechanical comparison of expandable cages for vertebral body replacement in the thoracolumbar spine. Spine 2004;29:1413–9.

[17] Kotani Y, Cunningham BW, Parker LM, Kanayama M, McAfee PC. Static and fatigue biomechanical properties of anterior thoracolumbar instrumentation systems: a synthetic testing model. Spine 1999;24: 1406–13.